Spectroscopic Study of Erythrosin B in PVA Films

Regien G. Stomphorst,*,† Gert van der Zwan,‡,§ Marc A. M. J. van Zandvoort,∥,⊥ Alexander B. Sieval,# Han Zuilhof,# Frank J. Vergeldt,† and Tjeerd J. Schaafsma†

Molecular Physics Group, Department of Biomolecular Sciences, Wageningen University, Dreijenlaan 3, 6703 HA Wageningen, The Netherlands, Department of Analytical Chemistry and Applied Spectroscopy, Vrije Universiteit, De Boelelaan 1083, 1081 HV Amsterdam, The Netherlands, Debye Institute, Department of Molecular Biophysics, Utrecht University, Princetonplein 5, 3584 CC Utrecht, The Netherlands, and Laboratory of Organic Chemistry, Wageningen University, Dreijenlaan 8, 6703 HB Wageningen, The Netherlands

Received: November 14, 2000; In Final Form: January 22, 2001

The effects of increasing concentration ($10^{-7}-2.5 \times 10^{-3}$ mol/g) of Erythrosin B (Ery B) in poly(vinyl alcohol) films on its visible absorption spectrum have been investigated. In a concentration range of $2 \times 10^{-7}-10^{-5}$ mol/g, no effects on the absorption spectrum are found. By contrast, within this concentration range, time-resolved fluorescence experiments (fluorescence and anisotropy decay) reveal the presence of energy transfer between Ery B molecules, followed by fluorescence at low concentrations and fluorescence quenching at higher concentrations. At a concentration of $\approx 5 \times 10^{-5}$ mol/g, the absorption spectrum broadens as compared to the monomeric spectrum and fluorescence is almost completely quenched. A further increase of the concentration results in a blue shift of the absorption spectrum. Using molecular mechanics calculations, it is shown that the initial broadening can be ascribed to excitonic interactions between randomly oriented molecules, whereas the blue shift at higher concentrations can be explained by the formation of oligomeric structures. At concentrations of $\geq 2.5 \times 10^{-3}$ mol/g, the molecules are closely packed, resulting in a contribution at the red edge of the absorption spectrum.

1. Introduction

Understanding the excitonic interactions between chromophores (pigment or dye molecules) and the consequences for their spectral behavior is essential to construct artificial antenna systems.[1−3] In natural photosynthetic systems, the chromophores are held in fixed relative orientations and distances, which are dictated by the proteins in which they are embedded. To create an artificial embedding for the dye molecules, one can conveniently make use of polymer matrixes.[4,5] Dye molecules in polymer films are more flexible in the way they organize themselves with respect to each other than chromophores embedded in proteins. The use of a polymer matrix avoids clustering of the dye molecules to aggregates that chromophores, such as chlorophylls or porphyrins, often display in water and organic solvents. However, in all randomly oriented systems, excitation energy gets lost by fluorescence and fluorescence quenching.[6] Fluorescence quenching is mostly attributed to energy transfer from excited monomers to quenching pairs[7,8] and already occurs at concentrations at which the majority of the molecules are still monomers as judged from the absorption spectra. Monomer-to-monomer energy transfer can be revealed by the fluorescence anisotropy decay of the acceptor molecules.[9] Monomer-to-dimer energy transfer can be investigated by fluorescence quenching. When excitonic interactions are affecting the absorption spectra, the first effect of these interactions is the broadening of spectra compared to the monomeric spectra, provided the intermolecular distances are sufficiently large to exclude a ground-state interaction(s), resulting in preferential orientations of neighboring molecules.[8] When the concentration is too high to permit the chromophore molecules to be randomly oriented, intermolecular steric hindrance between the molecules dictates their orientational distribution.

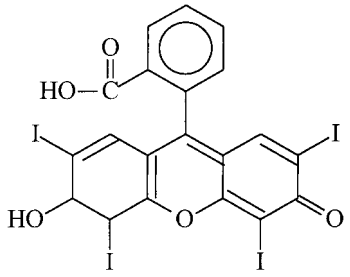

Figure 1. Molecular structure of Ery B.

This paper treats the spectral effects of increasing concentration of Erythrosin B (Ery B; Figure 1) molecules in PVA films. We measured absorption spectra to investigate the behavior of Ery B molecules in PVA films, using absorption and fluorescence spectroscopy and molecular mechanics computations to explain the spectral shifts and shapes of the absorption spectra at various chromophore concentrations. Because at low concentrations of Ery B the absorption spectra are not different from the monomeric spectra, we use the fluorescence lifetime

* To whom correspondence should be addressed. E-mail: regien@uuu.chem.vu.nl.
† Department of Biomolecular Sciences, Wageningen University.
‡ E-mail: zwan@chem.vu.nl.
§ Vrije Universiteit.
∥ Present address: Cardiovascular Research Institute Maastricht, Department of Biophysics, Universiteit Maastricht, P.O. Box 616, 6200 MD Maastricht, The Netherlands.
⊥ Utrecht University.
Laboratory of Organic Chemistry, Wageningen University.

10.1021/jp0041813 CCC: $20.00
Published on Web 04/04/2001

and anisotropy to investigate the intermolecular interactions between excited Ery B molecules at increasing concentration.

2. Materials and Methods

2.1. Sample Preparation. Dimethyl sulfoxide (DMSO; J. T. Baker Chemicals B. V., analytical grade) was used without further purification. Hydrolyzed (100%) poly(vinyl alcohol) (PVA; Aldrich Chemie) with an average molecular weight of 100 kD was purified from side products using a modified ethanol extraction method previously described.[10,11] Ery B (Merck) was used as received. PVA solutions in DMSO were prepared by adding 1 g of purified PVA powder to 12 mL of DMSO and heating this mixture to 353 K under continuous magnetic stirring until a clear solution was obtained. The PVA/DMSO solution was then mixed with the desired amount of the stock solution of Ery B in DMSO. For the preparation of the films, two preparation methods were used. In the first, the evaporation method, the solution was poured out on a small glass plate, followed by drying in the dark under a continuous nitrogen stream. For low concentrations of Ery B, this method results in $\approx$50 μm thick films, with sufficient optical absorption (OD $\geq$ 0.05). At higher Ery B concentrations, the films were made as thin as possible to prevent reabsorption effects (OD $\leq$ 0.5). Final Ery B concentrations in the films were in the range of 10^{-7}–2.5×10^{-3} mol/g PVA. The refractive index of PVA films was 1.52 as determined using an Abbe refractometer. No birefringence was observed. In the second method ,i.e., spin coating, the solution was poured on a small glass plate and subsequently spun around on a turning table, resulting in $\approx$50 μm layers. For time-resolved experiments, the films were placed between thin glass plates using ultrapure glycerol to ensure optical contact with the glass. The glass plates were glued around the edges and masked with black tape, leaving a spot of 2 mm in diameter for illumination.

2.2. Experiments. Time-resolved measurements of the fluorescence and fluorescence anisotropy decay of the films were carried out at the LENS Institute (Laboratorio di Spettroscopia Moleculare) in Florence (Italy) using the time correlated single photon-counting system,[12] at an excitation wavelength of 532 $\pm$ 1 nm. The fluorescence was observed through a band-pass interference filter with peak transmission at 573 nm and bandwidth of 6 nm (Omega) and a 550 nm cutoff filter (Omega). The fluorescence was collected in a quasiforward geometry, thus preventing the excitation beam from directly reaching the detection system. The instrumental function of the detection system was obtained for each measurement by measuring the time profile of the scattered laser light. For the present experimental conditions, its full width at half-maximum (fwhm) was 80 ps. Typically, decay curves were measured over 1000 channels with a width of 0.046 12 ns and a maximum peak of more than 2×10^4 counts for the sum ($I_{vv} + 2I_{vh}$). Because of the possibility of degradation of Ery B on heating and long exposure to the laser light, the photochemical stability of the sample was checked after each data run by measuring the absorption spectrum. No visible decomposition was found. Unpolarized absorption spectra were measured at room temperature using a DW2000 (SLM-Aminco) or a Kontron Uvicon 810 spectrophotometer. The slit widths were 2 nm on both spectrophotometers. No differences were detected between the results obtained with the two instruments.

2.3. Molecular Modeling. All calculations were done with the MSI program Cerius[2],[13] using the PCFF force field[14–17] and applying "high-convergence criteria"[18,19] in all minimizations. The geometry of a single Ery B molecule was optimized. Subsequently, this optimized molecule was used to construct clusters of two, three, and four Ery B molecules by copying and moving this structure. The initial positions and orientations of the Ery B molecules, which form the oligomers are important. Various interactions (e.g., $\pi-\pi$ stacking, COOH dimers, and hydrogen bonding between the OH and C=O groups of the molecules) are included in the calculations. The relative positions and orientations of the chromophores dictate the initial value of the strength of these interactions. A particular orientation of the monomer units in a dimer might give rise to a local minimum, which is not the lowest possible. The possible interactions were investigated by systematically varying the relative positions and orientations of the molecules in a cluster with respect to each other. The number of possible orientations grows rapidly with the number of molecules in a cluster, as a result of the different interactions between the monomers. Therefore it is necessary from a practical point of view to eliminate certain types of—chemically less relevant—structures from the calculations at an early stage. The more that molecules need to be considered, the more of the clusters that can be designed have a local energy minimum that may be considerably higher than that of the energetically lowest situation. Because it is not clear which types of structures should be eliminated, a deductive approach was used in the early stages of the investigations. As a rule of thumb, it was decided that if a certain orientation of the molecules gave an energy that was considerably lower (typically >10 kcal/mol) compared to the previous fully optimized situation (or ensemble of situations) from which it was derived the original needed no further investigation. The newly obtained geometry was then used as the new starting point. The same principle was used if the introduction of a new type of interaction gave similar differences in the energy of the system compared to that found for other types of interactions. By applying this method to several types of -chemically less realistic- orientations were eliminated at an early stage.

3. Calculation of Absorption Spectra

The excitonic interactions between the Ery B molecules depend on their mutual distance and orientation. Although because of ground-state interactions dimers, trimers, or even higher aggregates may be formed, the most probable distances between monomeric Ery B molecules in PVA films is calculated from their concentration. The distance between the molecules (R_0) is given by

$$R_0(nm) = \left(\frac{3 \times 10^{21}}{4\pi N_A 1.4 c_I}\right)^{1/3} \tag{3.1}$$

where N_A is Avogadro's number and c_I is the concentration of Ery B in PVA films, ranging from 10^{-7} to 2.5×10^{-3} mol/g. The density of the PVA films is 1.4 g/mL.[5] The most probable distance for a given monomer density is $\bar{R} = (^2/_3)^{1/3} R_0 \approx 0.87 R_0$ as follows from the nearest neighbor distribution.[8] The average distance of the nearest neighbor distribution (R_n) is[20]

$$<R_n> \approx 0.89 R_0 \tag{3.2}$$

Hence, the values between the most probable distance and the average value of the nearest neighbor distribution are not very different. Table 1 summarizes the R_0 values for the different concentrations. The length of an Ery B molecule is $\approx$0.7 nm. Consequently, for concentrations of 10^{-3} and 2.5×10^{-3} (and probably even 5×10^{-4}), steric hindrance affects the mutual orientation of the Ery B molecules in PVA films.

TABLE 1: Average Distance between Ery B Molecules vs Concentration

c (mol/g)	label	R_0 (nm)	c (mol/g)	label	R_0 (nm)
10^{-7}	A	14.1	10^{-4}	F	1.4
2×10^{-7}	B	11.3	5×10^{-4}	G	0.83
5×10^{-6}	C	3.8	10^{-3}	H	0.66
10^{-5}	D	3.1	2.5×10^{-3}	I	0.48
5×10^{-5}	E	1.8			

TABLE 2: Fluorescence and Fluorescence Anisotropy Decay Data

c (mol/g)	τ (ns)	r_0	$r(t)$ (ns)
10^{-7}	0.8 ± 0.1	0.37	
2×10^{-7}	0.8 ± 0.1	0.37	2.0
5×10^{-6}	0.5 ± 0.1	0.37	1.0
10^{-5}	0.4 ± 0.1	0.35	
5×10^{-5}	0.3 ± 0.1	0.33	

To simulate the absorption spectra, we use molecular exciton theory, assuming the point dipole approximation.[21,22] The excitonic interaction energy expressed by the interaction Hamiltonian $\hat{V}$ can be written as

$$\hat{V} = \frac{1}{4\pi\epsilon\epsilon_0 R^3}\hat{\vec{\mu}}_n \cdot \left(1 - 3\frac{\vec{R}_{n,m}\vec{R}_{n,m}}{R^2}\right)\cdot\hat{\vec{\mu}}_m \qquad (3.3)$$

where $\hat{\vec{\mu}}_n$ is the transition dipole operator of monomer n, ϵ is the relative dielectric constant of the solvent and $\vec{R}_{n,m}$ is the center to center distance between the molecules n and m. We use the quantity

$$V_0 \approx 5.035\frac{\mu^2}{\epsilon R^3}\ \mathrm{cm}^{-1} \qquad (3.4)$$

with μ in Debye units and R in nm, to scale the interactions. For Ery B molecules, the single dominant dipole moment is $\approx$6.3 D.[23] where ϵ for PVA was calculated to be 2.3, from the refractive index of 1.52. The distances R depend on the concentration considered (see eq 3.1). For a random distribution of Ery B molecules in PVA films, we can simulate the absorption spectra by assuming a distance distribution, letting the molecules adapt any mutual orientation with respect to each other and including inhomogeneous and homogeneous broadening.

To simulate the absorption spectra for the complex structures (dimers, trimers, and tetramers) as obtained from the molecular mechanics calculations, we analyzed the positions and orientations of the monomers contained in these complexes and we calculated the resulting stick spectra.[24] For realistic spectra, distance fluctuations and inhomogeneous and homogeneous broadening should be included. For our purpose only, the values of the stick spectra are relevant, because the spectral shift is our main interest.

4. Results

4.1. Spectroscopic Measurements. Table 2 contains the results of fluorescence and fluorescence anisotropy decay experiments. The decay curves were analyzed by using a reiterative deconvolution algorithm using a nonlinear least-squares Marquardt procedure and applying a multiexponential function to either the separate parallel and perpendicular fluorescence anisotropy decay curves I_{vv} and I_{vh} or the total intensity decay curve $I_{vv} + 2I_{vh}$. The first column of Table 2 presents the fluorescence lifetime τ (ns) for different concentrations of Ery B in PVA films. The second and last columns of Table 2 contain the initial anisotropy $r(0)$ and the anisotropy decay time t (ns). The absorption spectra for concentrations $\approx 5 \times 10^{-6}$ mol/g are shown in Figure 2. Next to the main B(0,0) band a second vibrational band is visible. Each spectrum is normalized at the peak value and consequently the surface area is not constant. Hence, the growth of the vibrational band is relative to these normalized peaks. In Table 1 and Figure 2, we labeled the different concentrations in alphabetic order.

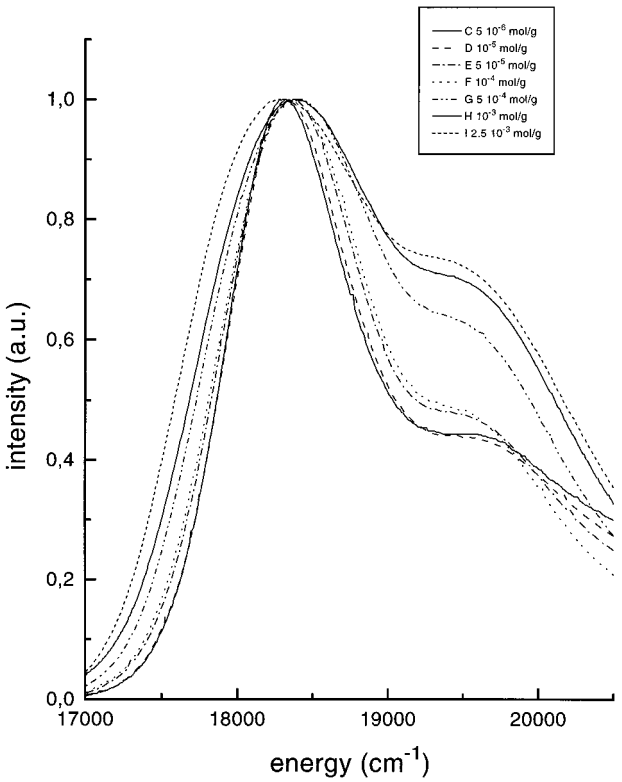

Figure 2. Absorption spectra for concentration range 5×10^{-6}–2.5×10^{-3} mol of Ery B/g of PVA.

4.2. Molecular Modeling. The formation of clusters is a possible explanation for the observed broadening and shifts of the absorption spectra. Therefore clusters of Ery B molecules were investigated by molecular mechanics calculations, using the MSI program Cerius[2] and the PCFF force field. This force field has been shown to be a suitable force field for the molecular modeling of clusters of (functionalized) organic molecules.[3,25] The optimized structures of the oligomeric clusters are shown in Figure 3. Table 3 shows the energies of these clusters and the distances between the monomers constituting these clusters, with reference to the structures in Figure 3 listed in the last column.

The results from the molecular mechanics calculations have shown that the Ery B molecules have various options for the formation of clusters or complexes. Calculations on dimeric complexes showed that the two dimers D1 and D2, in which a dimerization through the carboxylic acid groups occurs, are the most stable dimers. These two structures only differ in the relative orientation of the aromatic rings. The energy per Ery B molecule in these clusters (15.7 and 16.9 kcal/mol, respectively) is lower by $\approx$10 kcal/mol than that of a single Ery B molecule (26.8 kcal/mol). The formation of trimeric structures is enthalpically more favorable than dimerization. In the trimers Tri1 and Tri2, which are geometrically different but have the same energy per Ery B molecule (7.8 kcal/mol), the aromatic moiety of the third Ery B molecule is between the large aromatic

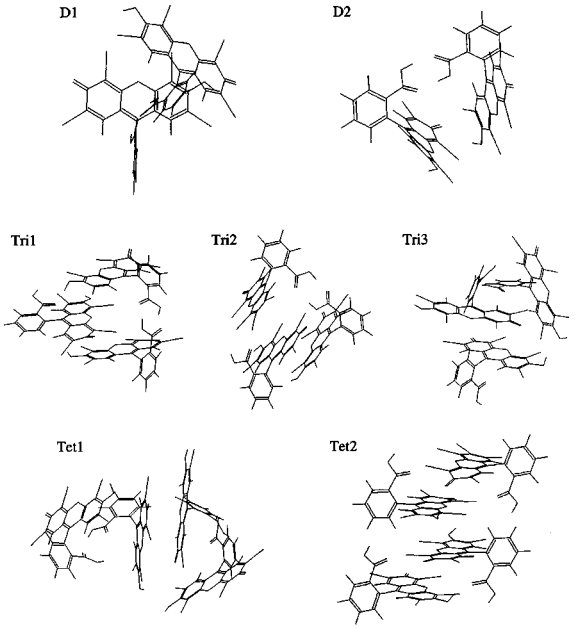

Figure 3. Energetically favorable optimized dimers, trimers, and tetramers according to PCFF molecular mechanics computations.

TABLE 3: Low Energy Structures Based on Molecular Mechanics Calculations

oligomer[a]	energy (kcal/mol)	distances (nm)	Figure 3
dimer 1	31.33	0.67	D1
dimer 2	33.76	0.60	D2
trimer 1	23.47	0.56; 0.63; 0.84	Tri1
trimer 2	23.48	0.59; 0.62; 0.78	Tri2
trimer 3	24.95	0.47; 0.71; 0.78	Tri3
tetramer 1	21.19	0.70; 0.47; 0.63[b]	Tet1
tetramer 2	21.90	0.53; 0.44; 0.57[b]	Tet2

[a] The monomer energy is 26.8 kcal/mol. [b] Nearest neighbor distances.

systems of the other two molecules, which strongly increases the $\pi-\pi$ interactions between the large aromatic rings. The "carboxylic acid" dimer in the collection of dimeric structures is not completely destroyed by this process. In the third trimeric structure, Tri3, which is only 1.5 kcal/mol higher in energy (i.e., 0.5 kcal/mol per Ery B molecule) compared to Tri1 and Tri2, the acid dimers are partially broken and a complex three-dimensional cluster has been formed, in which both $\pi-\pi$ interactions and interactions between the OH and C═O groups of the Ery B molecules are present. In all three trimers the energy per Ery B molecule is lower, by ≈8 kcal/mol, compared to the values as found for the dimers D1 and D2. This indicates that the enthalpy for formation of these trimeric structures is more favorable than dimerization. Formation of tetrameric structures even further decreases the energy of the system; however, the gain in energy per Ery B molecule is somewhat lower than for the dimer-to-trimer transition. The two structures with the lowest energy are depicted in Figure 3. For Tet1, a fourth Ery B molecule appears to bind to trimer Tri3. This molecule is at the left side in the picture of Tet1 and has formed a carboxylic acid dimer with the lowest Ery B molecule in Tri3. The structure of the former trimeric part shows only small differences compared to Tri3. In Tet2, the stacking of the aromatic moieties has become dominant and the dimers of the carboxylic acid groups have completely disappeared. The formation of larger clusters (pentameric, hexameric, etc.) is also possible, because this will still result in a lower enthalpy per Ery B molecule, given the trend that is present in Table 3. However, such structures were not investigated, because it becomes increasingly difficult to design the appropriate clusters that yield the global minimum because the number of possible interactions and combinations increases rapidly. As a result, the difference between the various situations will also become smaller and probably too small for these larger clusters, an effect that was already found for the tetramers. Although the formation of very large clusters might be favorable from the point of view of the enthalpy, the actual clustering may not occur as a result of entropy considerations, which are not incorporated in the calculations. For larger structures, the entropy contribution to the free energy becomes increasingly important, so molecular mechanics calculations cannot predict the stability of large molecular aggregates. The results of these molecular mechanics calculations show that enthalpy favors the formation of small Ery B clusters. Thus, it is expected that clustering will occur in the films. However, whether the clusters are actually formed depends not only on the gain in energy for each Ery B molecule in the cluster but also on other factors, such as the polarity of the local environment in the films and the kinetics of the complexation process, neither of which can be investigated by molecular mechanics calculations. Thus, it is not possible to predict from these results alone which clusters, dimers, trimers, or tetramers will actually be in the films. The simulated spectra for these structures are given in Table 4. As can be seen from this table, blue shifts are dominant.

TABLE 4: Calculated Spectra for Structures Given in Table 3

oligomer	energy blue shift (cm^{-1}; intensity)[a]	energy red shift (cm^{-1})
dimer 1	270 (82)	−270 (12)
dimer 2	200 (98)	−200 (2)
trimer 1	90 (25); 190 (70)	−280 (5)
trimer 2	90 (55); 170 (40)	−260 (5)
trimer 3	70 (38); 230 (38)	−300 (24)
tetramer 1	35 (28); 400 (49)	−35 (6); −400 (17)
tetramer 2	1300 (83)	−6 (9); −200 (7); −1094 (1)

[a] The relative intensity is given in parentheses.

5. Discussion

5.1. Concentration Range $10^{-7}-5 \times 10^{-5}$ mol/g: Fluorescence and Fluorescence Anisotropy Decay. First we discuss the results of the fluorescence- and fluorescence anisotropy decay experiments. The results given in Table 2 reveal the following: at the 10^{-7} mol/g concentration, the value of the initial polarization $R(0)$ agrees with published values[26] when no energy transfer takes place. The same applies to the constant value of the fluorescence anistropy. Both the absorption and the fluorescence spectra indicate the presence of monomers. At a concentration of 2×10^{-7} mol/g, the fluorescence anisotropy decay become noticeable because of energy transfer among the monomers. The initial value of the anisotropy and the fluorescence lifetime equal those of the monomers,[26] implying that the fluorescence is not quenched by oligomers. At a concentration of 5×10^{-6} mol/g, the fluorescence anisotropy decays faster as a result of more efficient energy transfer. Another new feature at this concentration is the decrease of the fluorescence lifetime, which implies that the quantum yield of the fluorescence has decreased. This is explained by energy transfer from an excited monomer to a nonfluorescent species, which leads to a faster fluorescence decay and a shortening of the flourescence lifetime.[4,27] In Part 1, the companion paper to this paper,[8] we

discussed the number of quenching pairs present vs the concentration. Under the assumption that monomers closer together than 1 nm form quenching pairs,[8] the probability to encounter a quenching pair is approximately 1%. At a concentration of 10^{-5} mol/g, the fluorescence quenching is further enhanced, yielding a further lifetime shortening and giving rise to a lower initial anisotropy. Already at this concentration the anisotropy decay is too fast to be experimentally observable. At a concentration of 5×10^{-5} mol/g, the probability to encounter a quenching pair has increased to 40% and the fluorescence quenching is further increased. At concentrations $\geq 5 \times 10^{-5}$ mol/g, the fluorescence is quenched beyond detection.

5.2. Concentration Range 5×10^{-5}−10^{-4} mol/g: Absorption Spectra. At concentrations $\leq 5 \times 10^{-6}$ mol/g, the absorption spectra are identical to those of the monomers. Note the B(0,1) vibrational band next to the main B(0,0) band (Figure 2). The noticeable growth of the B(0,1)/B(0,0) intensity ratio at higher concentrations (Figure 2) is mainly caused by broadening of the B(0,0) band, thereby lowering its intensity. In the remainder of this section, we concentrate on the B(0,0) band.

Between 5×10^{-5} and 10^{-4} mol/g the spectra start to exhibit a general broadening and a slight blue shift with respect to the monomeric spectra. The average intermolecular distance at these concentrations is calculated to be ≈1.5 nm, whereas the molecular size is ≈0.7 nm. This means that the majority of the molecules have sufficient freedom to adapt any mutual orientation. A fraction of ≈10% of the molecules are closer than 0.7 nm, however, and have limited freedom to rotate. The spectral shifts of molecules with an average intermolecular distance of ≈1.5 nm correspond to $V_0 = 20 - 50$ cm^{-1} (eq 3.3)

5.3. Concentration Range 10^{-4}−10^{-3} mol/g: Absorption Spectra. Whereas excitonic interactions between randomly oriented molecules cause only spectral broadening, simulated spectra using molecular mechanics calculations show that the formation of dimeric, trimeric, and tetrameric structures results in a blue shift (Table 4). At 5×10^{-4} mol/g, the average distance between the molecules is only slightly larger than the size of the molecules. Thus, we expect a number of the complex structures, including those presented in Figure 2, to be present in the films. This explains the clearly visible blue shift of the spectrum at a concentration of 5×10^{-4} mol/g. This spectrum shows that tetramer 2 does not appear to have a large contribution to the spectrum because its shift would have been located at 197 500 cm^{-1}, which is the location of the B(0,1) band, and apparently at that position there is no enhanced intensity. The detailed mechanism which determines the actually present structures is not clear. The energy differences between the various clusters are small, so it seems likely that a small difference in preparation conditions may change the fraction of each of the structures present in the film. This argument is supported by the results for spin-coated films (see next section), which produce different spectral shifts than discussed before. Also, for spin coated films, blue shifts remain dominant, however.

5.4. Concentration Range 10^{-3}−2.5×10^{-3} mol/g: Absorption Spectra. At concentrations of 10^{-3} and 2.5×10^{-3} mol/g, the chromophores are closely packed, i.e., at a concentration of 2.5×10^{-3} mol/g, 1 g of PVA contains 2.2 g of Ery B. The space to form isolated oligomer structures found at low concentrations is now considerably reduced. The resulting structures contain Ery B molecules parallel to each other and parallel to the connecting vector $\vec{R}$.

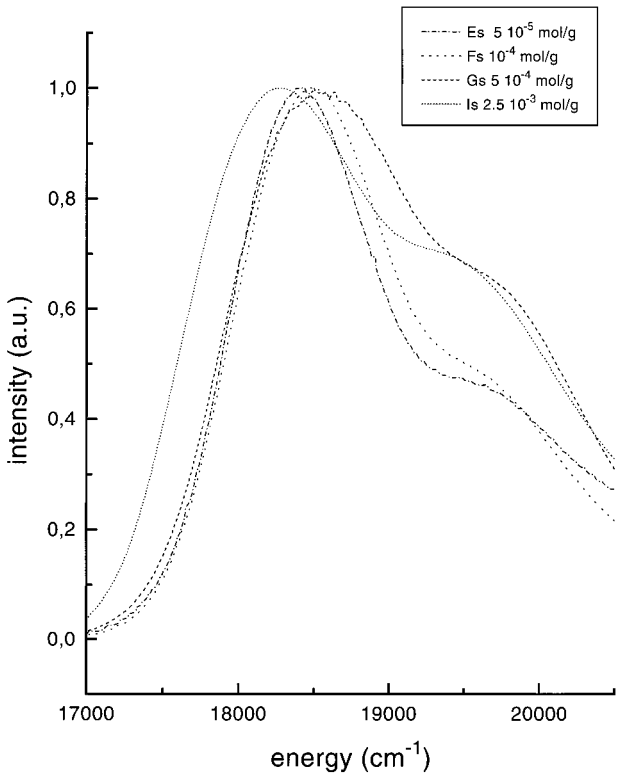

Figure 4. Absorption spectra for spin coated samples.

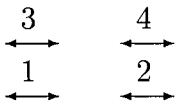

The exciton interactions between chromophores 1 and 2 cause red shifs. The same applies to chromophores 3 and 4. The angle between the connecting vector $\vec{R}$ of chromophores 1 and 4 and the chromophore transition dipole moments of these chromophores is below the magic angle, and hence, these combinations cause mainly red shifts. Only the combinations of 1 and 3 and 2 and 4 cause blue shifts. Hence, this very dense packing results in a spectral shift which is dominant to the red side of the spectrum.

5.5 Spin-Coating. At concentrations of 5×10^{-5}−2.5×10^{-3} mol/g, we also prepared some samples by applying spin coating instead of the drop evaporation technique (see Materials and Methods section). Spin-coating is frequently used to deposit thin layers (≤500 nm) on a substrate[28−30] and is carried out by spinning the sample at a constant speed during deposition of a small amount of dye solution. We expected that spin coating was an easier way to make thin films without strongly influencing the spectra, but as can be seen from a comparison of Figures 2 and 4, some spin-coated samples have spectra which are significantly different from those prepared by casting and evaporation (Figure 2). Spectra I and Is hardly differ, but spectra E, F, and G (evaporation method) and spectra Es, Fs, and Gs (spin coating method) are quite different. However, the last mentioned spectra are all blue shifted. It seems that the forces on the molecule during the spin coating process, cause differences in the orientation of the chromophores with respect to each other. Two different mechanisms, which could cause the difference between spin coated and evaporated samples are as follows:

(i) The individual oligomer structures are the same (see Figure 3), but the relative occurrence of each of these structures is different. To give an example, tetramer 2 seems hardly present

in evaporated samples but this might be the cause of the experimental blue shift at the location of the B(0,1) band in the spin-coated sample at a concentration 5×10^{-4} mol/g.

(ii) The strong shear forces applied on the spin-coated samples cause the chromophores to align, giving them a different orientation than with casting/evaporation.

Whatever mechanism might work, it is important to realize that the spin-coating and evaporation method could give different absorption spectra caused by different molecular structures. Because at the highest concentration of 2.5×10^{-3} mol/g films prepared by spin-coating and casting/evaporation have the same red-shifted spectral profile, one may conclude that at this high concentration the aggregate structure is predominantly determined by the properties of the Ery B molecules themselves and not by external forces, such as occur during spin-coating. At intermediate concentrations, the dye molecules have freedom to yield their orientation to the highly anisotropic forces during spin-coating.

6. Conclusions

1. The effects of concentration on the absorption spectrum of Ery B in PVA films are not observable at low concentrations ($\leq 5 \times 10^{-5}$ mol/g), but fluorescence anisotropy decay experiments demonstrate the presence of quenching of excited monomers by concentration pairs in their immediate environment.

2. At concentrations $\geq 5 \times 10^{-5}$ mol/g, excitonic interactions between Ery B molecules become noticeable in the absorption spectrum. In the concentration range 5×10^{-5}–2.5×10^{-3} mol/g, broadening of the spectra is first observed, then a blue shift, and finally a red shift of the spectra at the highest concentration.

Acknowledgment. The authors want to thank R. Torre and P. Bertolini at the LENS Institute in Florence for their help with time-resolved measurements.

References and Notes

(1) Kroon, J. M.; Südholter, E. J. R.; Wienke, J.; Koehorst, R. B. M.; Savenije, T. J.; Schaafsma, T. J. In *Proceedings of the 13th European Photovoltaic Solar Energy Conference*; 1995; pp 1295−1298.

(2) Calzaferri, G. *Proc.−Indian Acad. Sci., Chem. Sci*. **1997**, *109* (6), 429.

(3) Struijk, C. W.; Sieval, A. B.; Dakhorst, J. E. J.; Kimkes, P.; Zuilhof, H.; Sudhölter, E. J. R.; Koehorst, R. B. M.; Donker, H.; Schaafsma, T. J.; Picken, S. J.; Van de Craats, A. M.; Warman, J. M. *J. Am. Chem. Soc.* In press.

(4) Van Zandvoort, M. A. M. J. Pigment-polymer matrixes as model systems for energy transfer processes between photosynthetic piments, Ph.D. Thesis, University of Utrecht, 1994.

(5) Van Zandvoort, M. A. M. J.; Wróbel, D.; Lettinga, P.; van Ginkel, G.; Levine, Y. K. *Photochem. Photobiol.* **1995**, *62*, 279.

(6) Beddard, G. S.; Porter, G. *Nature* **1976**, *260*, 366.

(7) Knox, R. S. *J. Phys. Chem.* **1994**, *98*, 7270.

(8) Stomphorst, R. G.; Schaafsma, T. J.; Van der Zwan, G. *J. Phys. Chem. A* **2001**, *105*, 4226.

(9) Lettinga, M. P.; Zuilhof, H.; Van Zandvoort, M. A. M. J. *Phys. Chem. Chem. Phys.* **2000**, *2*, 3697.

(10) Van Zandvoort, M. A. M. J.; Wróbel, D.; Scholten, A. J.; de Jager, D.; van Ginkel, G.; Levine, Y. K. *Photochem. Photobiol.* **1993**, *58*, 600.

(11) Haas, H. C.; Husek, H.; Taylor, L. D. *J. Polymer. Sci., Part A: Gen. Pap.* **1963**, *1*.

(12) Arcioni, A.; Van Zandvoort, M. A. M. J.; Bartolini, P.; Torre, R.; Tarroni, R.; Righini, R.; Zannoni, C. *J. Phys. Chem. B* **1998**, *102*, 1624.

(13) Cerius^2, version 3.8; Molecular Simulations Inc. 1998.

(14) Sun, H.; Mumby, S.; Maple, J. R.; Hagler, A. T. *J. Phys. Chem.* **1995**, *99*, 5873.

(15) Sun, H. *Macromolecules* **1995**, *28*, 701.

(16) Hill, J. R.; Sauer, J. *J. Phys. Chem.* **1998**, *98*, 1238.

(17) Hwang, M. J.; Stockfisch, T. P.; Hagler, A. T. *J. Am. Chem. Soc.* **1994**, *116*, 2515.

(18) This term is specific to the Cerius^2 program, so it has in the text been put between quotes.

(19) The criteria for the high-convergence minimizations are as follows: atom root-mean-square force 1×10^{-2} kcal mol^{-1} nm^{-1}; atom maximum force 5×10^{-2} kcal mol^{-1} nm^{-1}; energy difference 1×10^{-4} kcal/mol; root-mean-square displacement 1×10^{-6} nm; maximum displacement 5×10^{-6} nm.

(20) Hertz, P. *Math. Ann.* **1908**, *67*, 387.

(21) Kasha, M.; Rawls, H. R.; Ashraf El-Bayoumi, M. *Pure Appl. Chem.* **1965**, *11*, 371.

(22) McRae, E. G.; Kasha, M. J. *Chem. Phys.* **1958**, *28*, 721.

(23) The dipole moment has been calculated using the extinction coefficient of 10^5 mol^{-1} cm^{-1} and an estimate for the full width at half-maximum of 770 cm^{-1} at peak maximum of 18 300 cm^{-1}. The last two values were estimated by fitting the monomeric absorption spectra (see Figure 2) with separate Gaussian line shapes for the B(0,0) band and the B(0,1) band. Only the B(0,0) band has been taken into consideration.

(24) Stomphorst, R. G.; Koehorst, R. B. M.; Van der Zwan, G.; Benthem, B.; Schaafsma, T. J. *J. Porphyrins Phthalocyanines* **1999**, *3*, 346.

(25) Sieval, A. B.; Van Hout, B.; Zuilhof, H.; Südholter, E. J. R. *Langmuir* **2000**, *16*, 2987.

(26) Lettinga, M. P.; Van Zandvoort, M. A. M. J.; Van Cats, C. M.; Philipse, A. P. *Langmuir* **2000**, *16* (15), 6156.

(27) Knoester, J. Incoherent energy transfer in disordered systems, Ph.D. Thesis, Utrecht University, 1987.

(28) Kerp, H.; Donker, H.; Koehorst, R. B. M.; Schaafsma, T. J.; Van Fraassen, E. E. *Chem. Phys. Lett.* **1998**, *298*, 312.

(29) Critchley, S. M.; Willis, M. R.; Cook, J.; McMurdo, J.; Maruyama, Y. *J. Mater. Chem.* **1992**, *2* (2), 157.

(30) Gregg, B. A. *Chem. Phys. Lett.* **1996**, *258*, 376.